Supplemental Material

Massimiliano Chiappini, Eric Grelet, and Marjolein Dijkstra

(Dated: January 30, 2020)

I. COMPUTATIONAL METHODS

We model the experimental mixture of host and guest fd-viruses as a binary mixture of hard spherocylinders. We perform Monte Carlo simulations on a binary mixture of $N_h = 3072$ host rods of length L_h and diameter d and $N_g = 6$ guest rods of length L_g and diameter d. We use a high-density ABC crystal state as our initial configuration, and we expand the system via Monte Carlo (MC) simulations in the NPT ensemble to a low-density smectic state at pressure $\beta P v_0 \approx 6.39$ with a smectic layer spacing $\lambda \sim 1.1 L_h$. We keep the number of particles, N_g and N_h, the pressure P, and the temperature T fixed in the NPT MC simulation, whereas the system volume V and the particle configurations (positions and orientations) are evolved via random variations that are either accepted or rejected according to the acceptance rules that enforce the correct statistical physics [1].

After equilibration of the system, we perform production runs in the NVT ensemble, i.e. the number of particles N, volume V, and hence the density $\rho = N/V$ are kept fixed, and we track the positions of 3000 host particles and 6 guest particles to measure their diffusive properties. In general, MC simulations are not guaranteed to yield realistic particle trajectories, and do not provide a physical time scale. However, for sufficiently small maximum displacements NVT-MC simulations with simple translational and rotational moves produce trajectories that follow the correct Brownian dynamics. In the case of anisotropic particles, the maximum displacements have to be tuned according to the self-diffusion properties of each particle in order to enforce the correct anisotropy of the dynamics. More specifically, for rod-like particles, the ratio between the maximum displacements parallel and perpendicular to the particle axis $\delta_\parallel/\delta_\perp$ has to be equal to the ratio between the parallel and perpendicular diffusion coefficients at infinite dilution $D_{0,\parallel}/D_{0,\perp}$ [2].

In this Letter, we study the dynamic behavior of guest rods in a host smectic environment parallel to the nematic director $\hat{\mathbf{n}}$. However, reaching the long-term diffusive regime of highly anisotropic particles in a smectic phase is a highly non-trivial computational effort. In order to reach and explore the long-term regime of the longitudinal dynamics of guest particles in a reasonable computational time, we increase the ratio between the parallel and perpendicular maximum displacements to speed up the parallel diffusion relative to the perpendicular one. Here, we assume that the parallel and perpendicular dynamics can be decoupled, *i.e.* that the perpendicular diffusive behavior has a negligible effect on the parallel diffusion. In

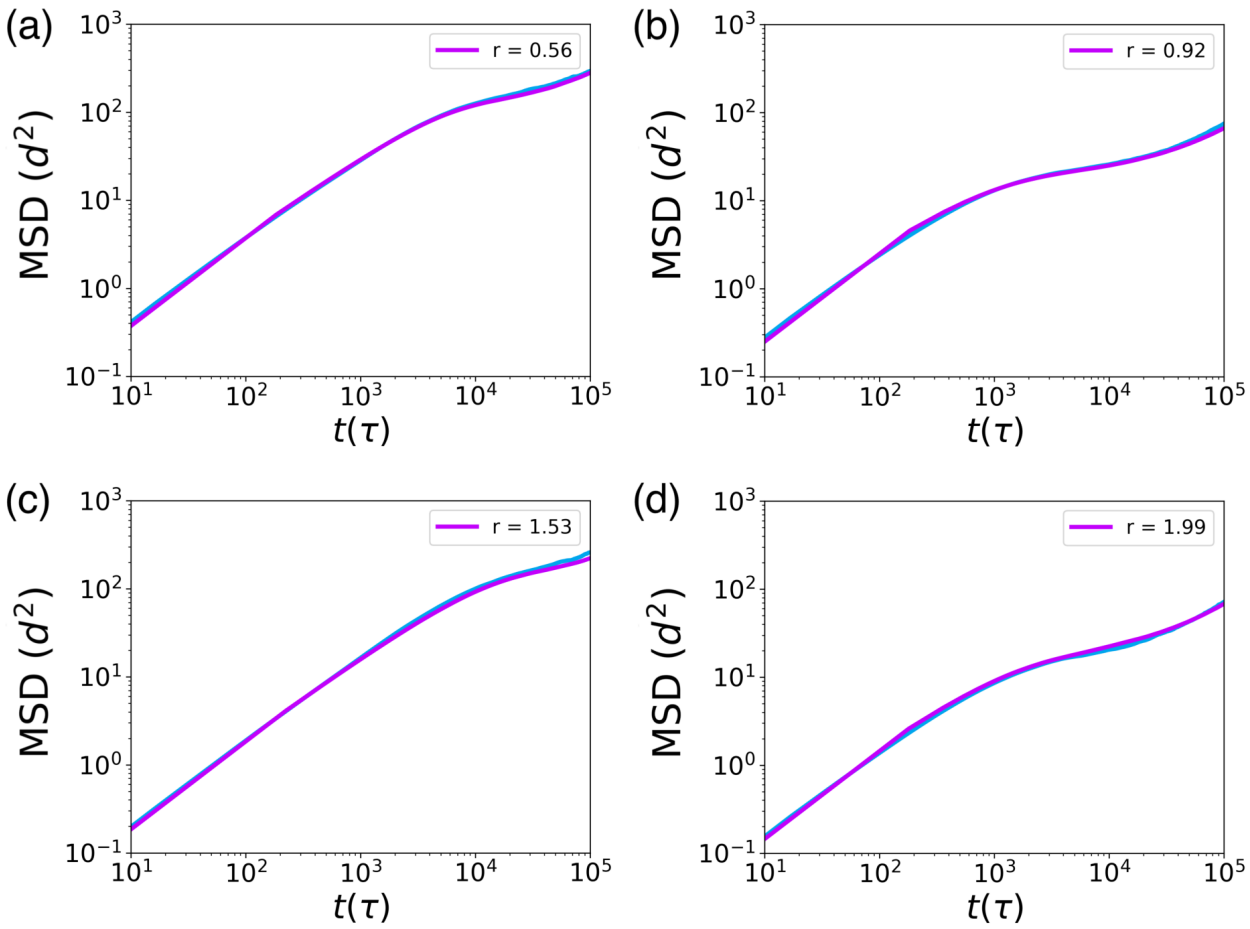

FIG. S1. Parallel MSDs (along the long rod axis) in the smectic-A phase from basic MC simulations (in purple) after rescaling onto the MSDs from DMC simulations (in blue) for size ratios $r = 0.56$ (a), 0.92 (b), 1.53 (c), and 1.99 (d).

particular, we set $\delta_\perp = 0.08d$ and $\delta_\parallel = 5\delta_\perp = 0.4d$, and we find that for these values of the maximum displacements, MC simulations consisting of $\sim 1.5 \cdot 10^8$ MC cycles are sufficient to reach and adequately sample the long-term diffusive behavior. In particular, we save the positions of the tracked host and guest particles every 10^3 MC steps, hence producing trajectories of $N_t \sim 1.5 \cdot 10^5$ points.

We measure the MSD at discrete times $t \in [1, N_t]$ using N_g trajectories $z_i = [z_{i,1}, z_{i,2}, \ldots, z_{i,N_t}]$ as

$$MSD(t) = \frac{1}{N_g} \sum_{i=1}^{N_g} \frac{1}{(N_t - t)} \sum_{j=1}^{N_t - t} \left(z_{i,(j+t)} - z_{i,j} \right)^2 . \tag{1}$$

In order to determine the long-term diffusion coefficient $D_\parallel$, we consider a wide collection of time windows $\{[t_0, t_1]\}$ in the long-time diffusion limit of the MSD. In each time window,

we perform a fit of the MSD with $\gamma = 1$, and measure the reduced χ^2. Subsequently, we average the values of D of all time windows for which χ^2 is smaller than a certain threshold value. The statistical error on D is determined as the standard error on the average, and is of about the symbol size or smaller as indicated in Fig. 2 of the letter.

To test the validity of our assumption on the decouping of the parallel and perpendicular dynamics, we compare the MSDs from our MC simulations and the ones from simulations performed using the Dynamic Monte Carlo (DMC) method introduced by Patti and Cuetos [3]. In the DMC method, the maximum displacements of both translational and rotational motions are carefully tuned according to the diffusive properties of the particles at infinite dilution, resulting in reliable Brownian dynamics with respect to a physical unit of time $\tau = \mu\sigma^3/k_BT$, where μ is the solvent viscosity, σ the characteristic unit of length in the system and T the solvent temperature. We note that in the case of a binary mixture (as our guest/host particles mixture) a specific treatment is required as discussed in Ref. [4]. For every length of our guest particle that we consider, we perform an additional simulation with the more accurate but slow DMC method. Subsequently, we map the short-time MSDs from our basic MC simulations onto the ones from DMC simulations by rescaling the unit of time. If this mapping is accurate, the dynamics using the basic MC simulations is sufficiently reliable, and the rescaling of time onto the physical time unit τ can be used to compare the dynamical properties with experiments. In Fig. S01 we show typical examples of such a rescaling for varying size ratios $r = (L_g + d)/\lambda$ of the guest rods with λ the smectic layer spacing confirming the good mapping between the two approaches.

II. COMPUTATIONAL AND EXPERIMENTAL TIMES

In Fig. 1b of the Letter, we compare typical longitudinal trajectories of host and guest particles from simulations and experiments on the same time scale. However, matching the experimental and computational time scales is non-trivial, and deserves some discussion.

In the Section above we already showed that the mapping of the MSDs obtained from basic MC simulations onto DMC simulations provides a physical time unit $\tau = \mu\sigma^3/k_BT$, where μ is the solvent viscosity, σ the unit of length, and T the solvent temperature. In the experiments of Ref. [5], the particles are dispersed in water at room temperature, for which $\mu = 10^{-3}$ Pa $\cdot$ s and $k_BT = 4.11 \cdot 10^{-21}$ J. In our simulations, we use the particle diameter

d as our unit of length, and hence in the experimental system σ corresponds to the effective diameter $d_{eff} \sim 20$ nm of the fd viruses, where we have taken into account the electrostatic repulsion between the charged viruses [6]. This results in a conversion factor $\tau \approx 2 \cdot 10^{-6}$ s.

To test this conversion factor, we perform DMC simulations of single particles and measure their infinite dilution diffusion coefficient $D_0^{sim} = 1.16 \cdot 10^{-2} d^2/\tau$. Theoretically, the diffusion coefficient D_0^{th} of long rods ($L/d \ggg 1$) at infinite dilution is known and is expressed as [2]:

$$D_0^{\text{th}} = \frac{k_B T}{3\pi\mu L} \ln\left(\frac{L}{d}\right). \tag{2}$$

This yields for rods with an aspect ratio of $L/d \sim 40$, a diffusion coefficient $D_0^{\text{th}} = 2.3\ \mu\text{m}^2/\text{s}$, which is in quantitative agreement with $D_0^{\text{exp}} \approx 2\mu\text{m}^2/\text{s}$ experimentally measured in very dilute filamentous virus suspensions. Considering that $d = 20$ nm, with $\tau = 2 \cdot 10^{-6}$ s, we obtain $D_0^{sim} = 2.3\ \mu\text{m}^2/\text{s} = D_0^{\text{th}} \approx D_0^{\text{exp}}$, confirming the value of our conversion factor.

III. CAGING TIMES

As discussed in the Letter, the typical longitudinal MSD of a rod-like particle in a smectic environment is characterised by a cage-trapping plateau in between the short- and long-time diffusion regimes. We measure the extent of the caging effect upon varying the size ratio r of the guest particle with respect to the smectic layer spacing. Given the MSD across the three timescales for a given particle length, we perform three separate fits of the short-, intermediate-, and long-time regimes of the MSD. At short and long times, we fit the MSD with the theoretical expression for diffusive dynamics, $\text{MSD}(t) = 2Dt$, whereas at intermediate time we fit it with the expression for subdiffusive dynamics, $\text{MSD}(t) = 2Dt^\gamma$ with $\gamma < 1$. From the interception points between the fits at short and intermediate times, and the fits at intermediate and long times, we estimate the typical caging time δt, as shown in Fig. S02.

In Fig. S03 we report the caging time δt as a function of size ratio r. It clearly shows the opposite trend as the diffusion coefficients shown in the inset of Fig. 3 of the Letter, confirming the relationship between the shrinking of the caging plateau and the speeding up of the dynamics.

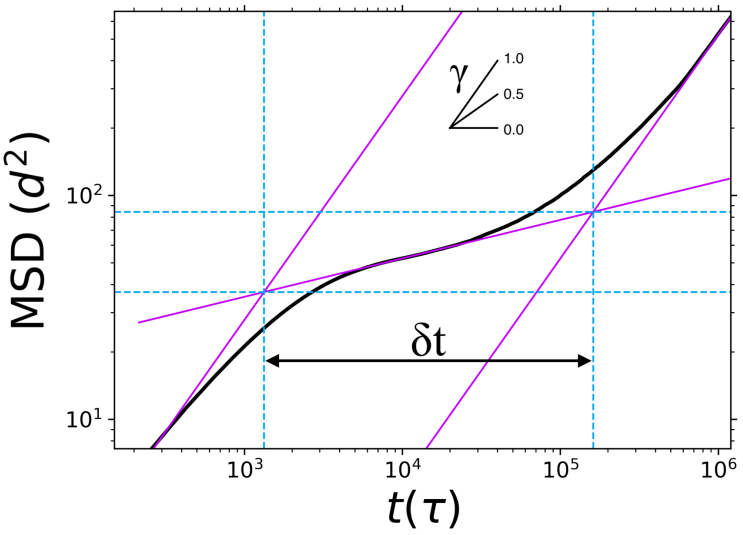

FIG. S2. MSD (in black) of guest rods with a size ratio $(L_g + d)/\lambda = 0.73$ in a host smectic environment with a smectic layer spacing λ with fits (in purple) of the short-, intermediate-, and long-time diffusion regimes. From the intercepts of the fits, we identify the time regimes in which the dynamics switches between short-time diffusion to an intermediate-time caged sub-diffusion with a caging time δt, to a long-time diffusion.

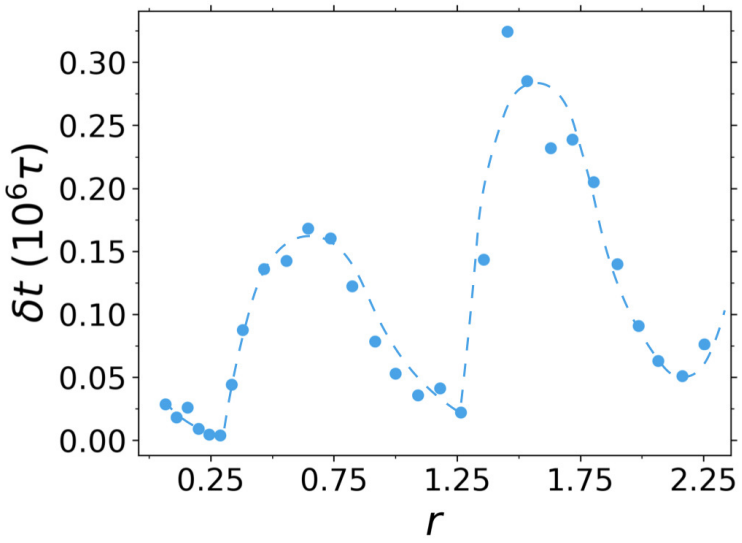

FIG. S3. Caging times δt as a function of the size ratio $r = (L_g + d)/\lambda$ of the guest particles. The dashed line is a guide to the eye.

IV. ADSORPTION TO THE INTERFACE OF THE SMECTIC LAYERS

Most of the smectic potentials presented in the Letter have a characteristic shape with two minima, implying that guest particles have two equilibrium positions (regime II). In particular, as shown in the Letter, these minima correspond to positions in which either one of the particle ends is adhered to the interface of a smectic layer.

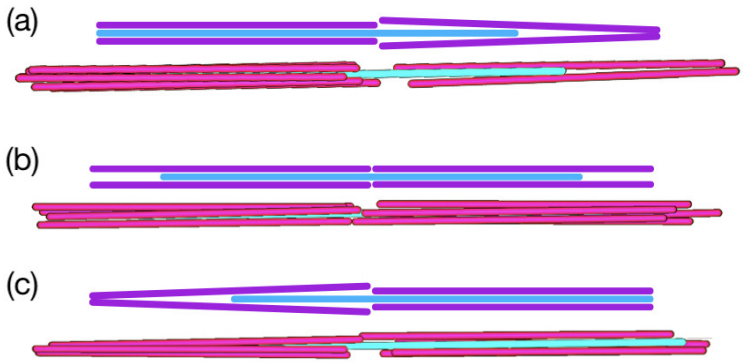

FIG. S4. Sketches (top) and snapshots from actual simulations (bottom) of a guest particle of length $L_g = 1.5L_h$ (corrisponding to a size ratio $r \sim 1.36$) and its neighbour host particles (whose centre of mass is contained in a cylinder of diameter $3D$ and height 3λ around the guest particle). When the guest particle adheres to an interface between layers (a and c) the voids created in the adjacent layer are wide enough for host particles to occupy it and to hinder the diffusion of the guest particle. Vice versa, when the particle sits in the center of a smectic layer (b), it creates two voids which are too small to be populated by host particles and hence the guest particle can diffuse away freely.

Fig. 4a-f of the main text shows that the two minima $z_1^{\min}$ and $z_2^{\min}$ of the effective potentials are separated by two potential barriers located at $z = n\lambda$ (barrier A) and $z = (n + 1/2)\lambda$ (barrier B). Monomers and "odd" multimers with $r \sim (2n + 1)$ feel exclusively the barriers at $z = n\lambda$, and dimers and "even" multimers with $r \sim (2n + 2)$ experience only the barriers at $z = (n + 1/2)\lambda$. As shown in Fig. S5a, guest particles in regime I experience exclusively the same barrier as the preceding multimer, whereas in regime III they only feel the same barrier as the successive multimer. In regime II, the dynamics of the guest rods is affected by both barriers and switches from a "monomer"-like to a "dimer"-like behavior upon changing r. Interestingly, in Fig. S5b we find that the sum of the barriers, accounting for the total smectic caging felt by the guest particle, is minimal for $r \sim n + 0.25$, for which

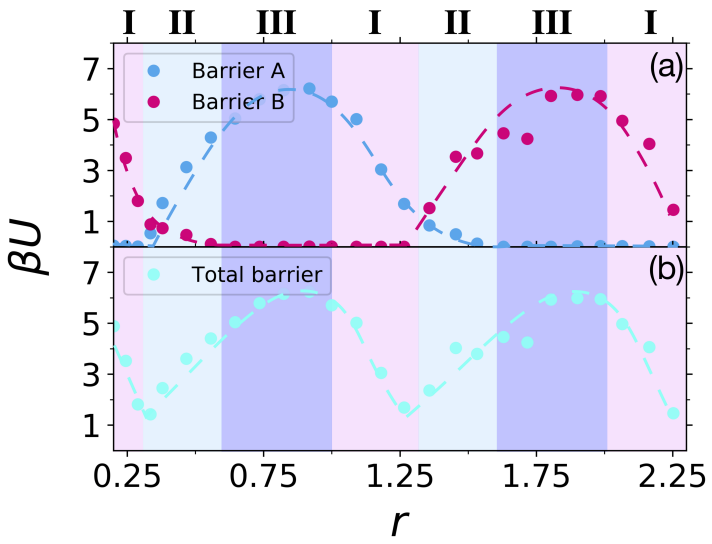

FIG. S5. (a) Height and (b) sum of the two potential energy barriers as a function of the size ratio r for guest rods in a host smectic phase. The background is colored according to the three diffusive regimes. Dashed lines are guides to the eye.

the fastest dynamics is observed, and maximal for $r \sim n + 0.75$, when the slowest dynamics is achieved, confirming that the dynamic behavior of guest rods in a host smectic phase can be rationalized in terms of the caging due to the lamellar environment

[1] D. Frenkel and B. Smit, *Understanding molecular simulation: from algorithms to applications* (Elsevier, 2001).

[2] M. M. Tirado and J. G. de la Torre, The Journal of Chemical Physics **71**, 2581 (1979).

[3] A. Patti and A. Cuetos, Phys. Rev. E **86**, 011403 (2012).

[4] A. Cuetos and A. Patti, Phys. Rev. E **92**, 022302 (2015).

[5] L. Alvarez, M. P. Lettinga, and E. Grelet, Phys. Rev. Lett. **118**, 178002 (2017).

[6] E. Grelet, Phys. Rev. X **4**, 021053 (2014).